

Cyril Fischer; Jiří Náprstek

Identification of quasiperiodic processes in the vicinity of the resonance

In: Jan Chleboun and Pavel Kůs and Jan Papež and Miroslav Rozložník and Karel Segeth and Jakub Šístek (eds.): Programs and Algorithms of Numerical Mathematics, Proceedings of Seminar. Jablonec nad Nisou, June 19-24, 2022. Institute of Mathematics CAS, Prague, 2023. pp. 57–64.

Persistent URL: <http://dml.cz/dmlcz/703188>

**Terms of use:**

Institute of Mathematics of the Czech Academy of Sciences provides access to digitized documents strictly for personal use. Each copy of any part of this document must contain these *Terms of use*.



This document has been digitized, optimized for electronic delivery and stamped with digital signature within the project *DML-CZ: The Czech Digital Mathematics Library*  
<http://dml.cz>

## IDENTIFICATION OF QUASIPERIODIC PROCESSES IN THE VICINITY OF THE RESONANCE

Cyril Fischer, Jiří Náprstek

Institute of Theoretical and Applied Mechanics of the CAS, v. v. i.  
Prosecká 76, Prague 9, Czech Republic  
{fischerc,naprstek}@itam.cas.cz

**Abstract:** In nonlinear dynamical systems, strong quasiperiodic beating effects appear due to combination of self-excited and forced vibration. The presence of symmetric or asymmetric beatings indicates an exchange of energy between individual degrees of freedom of the model or by multiple close dominant frequencies. This effect is illustrated by the case of the van der Pol equation in the vicinity of resonance. The approximate analysis of these nonlinear effects uses the harmonic balance method and the multiple scale method.

**Keywords:** dynamical systems, quasiperiodic response, van der Pol equation

**MSC:** 37C60, 37N05, 70G60, 34A12

### 1. Introduction

The frequency lock-in effect occurs, e.g., when an elastic profile vibrates in buffet-ing flow. It is characterised by the fact that the vibration frequency does not follow the vortex shedding frequency but locks onto the natural frequency of the profile. Such behaviour is illustrated in Fig. 1a, see [6], where the linear dependence of the frequency ratio on the stream velocity (which directly relates to the vortex shedding frequency) is interrupted at the ratio 1 for a non-negligible wind velocity interval.

This lock-in effect is usually modelled using the van der Pol equation, which corresponds to a single-degree-of-freedom (SDOF) physical system representing a circular bar in an air flow, see Fig. 1b. The spring in the SDOF model is considered linear, the damping term has the (quadratic) van der Pol character. The flow around the body induces a regular vortex shedding that is, in general, perturbed by a random pressure fluctuations.

The measured response in the lock-in region and its neighbourhood consists of the following cases, cf. also Fig. 1a: (a) small stationary amplitudes; the velocity is lower than the critical velocity and the vortex-shedding frequency is lower than the natural frequency; (b) the lock-in regime, a stationary vortex-induced resonance, maximal

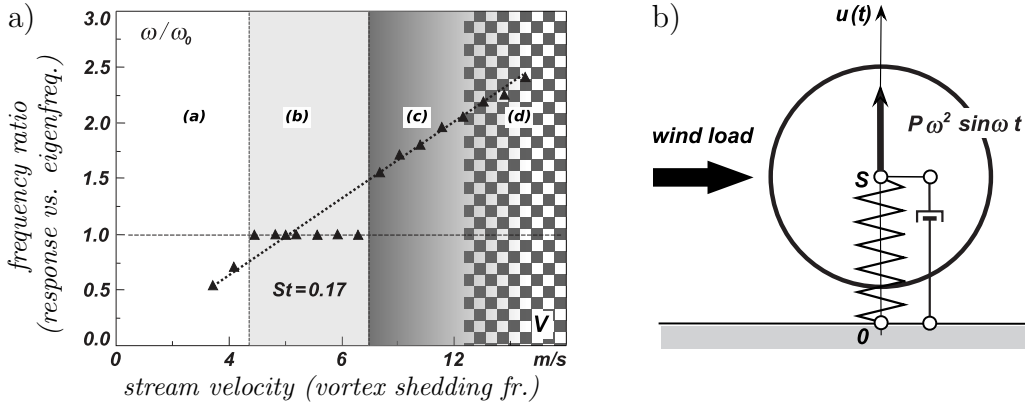


Figure 1: a) frequency ratio vs. the flow velocity and the lock-in domain; b) scheme of the SDOF model, [6]

amplitudes; (c) large beating amplitudes, caused by a small detuning of the forcing and natural frequencies outside the lock-in region; (d) small non-stationary post-critical vibrations of forced (non-resonant) vibrations caused by vortex shedding with a frequency larger than the natural frequency. The transition between regions (c) and (d) is not sharp; the influence of the natural frequency decays exponentially with increasing distance from the boundary of the lock-in region (b).

The case (c), i.e., the regime in the neighbourhood of the stationary lock-in, is studied in this contribution. The beating effect is caused by multiple close dominant frequencies which are present in the response. When a small random component is also present, the response has a character of a cyclostationary process [2].

This paper, as part of a larger project, restricts itself to the behaviour of the van der Pol equation solution under deterministic harmonic excitation in a region that is closely adjacent to the lock-in region. The general mathematical model presented in Section 2 is further studied numerically in Sect. 2.1, using the ‘‘harmonic balance’’ method (Sect. 2.2) and the ‘‘multiple scales’’ method (2.3).

## 2. Mathematical model

Vibration of a slender structure in an airflow is usually modelled using the van der Pol equation with a harmonic right hand side:

$$\ddot{u} - (\eta - \nu u^2)\dot{u} + \omega_0^2 u = P\omega^2 \cos \omega t + h \cdot \xi(t). \quad (1)$$

In Eq. (1),  $u(t)$  – displacement [m],  $\dot{u}(t)$  – velocity [ $ms^{-1}$ ],  $\eta, \nu$  – parameters of the damping [ $s^{-1}, s^{-1}m^{-2}$ ],  $\omega_0$  – eigen-frequency of the adjoint linear SDOF system,  $\omega$  – excitation frequency of the vortex shedding [ $s^{-1}$ ],  $P\omega^2$  – amplitude of the harmonic excitation (acceleration) [ $ms^{-2}$ ],  $h$  – multiplicative constant [ $ms^{-2}$ ],  $\xi(t)$  – stationary Gaussian random process [1]. In the rest of the paper,  $h = 0$  is assumed.

When regarded as a dynamical system, the solution exhibits one stable limit cycle, the rest position  $u(t) = 0$  is unstable.

## 2.1. Numerical analysis

For the first view, the stationary/non-stationary character of the solution to (1) can be analysed numerically in the frequency domain. Figure 2 shows the Fourier analysis of the set of responses obtained for the frequency range near the resonance frequency  $\omega_0 = 1$ . The dominant peaks of the periodogram for each value of  $\omega$  are plotted vertically. This way, the ordinate represents the Fourier frequency coefficients present in the response. The color intensity shows the absolute values of the dominant Fourier coefficients on a logarithmic scale. The detuning on the abscissa is defined as  $\Delta = \frac{\omega_0^2 - \omega^2}{2\omega}$ . The stationary lock-in interval of the harmonic response appears for  $-0.1 \lesssim \Delta \lesssim 0.12$ , although there are clearly two superharmonic components ( $\omega = 3\omega_0, 5\omega_0$ ). The complex behaviour of the nonlinear response is evident from the existence of a subharmonic resonance interval for negative  $\Delta$  (i.e., for  $\omega \approx 1/3$ ).

The most important aspect for this work is the behaviour at the boundaries of the lock-in intervals. There the dominant frequencies divide into a series of close but distinct frequencies that cause the beating character of the response. Their mutual distances increase rapidly with increasing distance from the lock-in region and cause shortening of the beating periods in the response. It is clear from this that the monochromatic representation of the solution used in the remaining text is only approximate and more accurate estimates will need to be used in the future.

## 2.2. Analysis based on the harmonic balance

Following the more general approach by the authors in [5], for a weak excitation force and a small detuning, the response can be expected to have an approximately harmonic form with slowly varying amplitude  $U(\tau)$  and phase  $\varphi(\tau)$ ,  $\tau = \varepsilon t, \varepsilon \ll 1$ :

$$u \rightarrow U(\tau) \cos(\omega t + \varphi(\tau)). \quad (2)$$

The *harmonic balance* procedure consists in multiplying Eq. (1) by  $\sin \omega t$  or  $\cos \omega t$  and subsequent integration over one period  $t \in (0, 2\pi/\omega)$ . Since  $(\tau)$  is “slow time”, the variability of  $U$  and  $\varphi$  within one period can be neglected and both functions can be treated as constants. Then:

$$\dot{U} = \frac{1}{2}U \left( \eta - \frac{1}{4}\nu U^2 \right) - \frac{1}{2}P\omega \sin \varphi, \quad (3a)$$

$$\dot{\varphi} = \Delta - \frac{1}{2U}P\omega \cos \varphi, \quad (3b)$$

where  $\Delta = \frac{\omega_0^2 - \omega^2}{2\omega} \approx \omega_0 - \omega$  and the derivative  $\dot{U}, \dot{\varphi}$  is taken with respect to  $\tau$ . The stationary amplitude for  $\dot{U} = 0, \dot{\varphi} = 0$  is given by

$$U^2 \left( 4\Delta^2 + \left( \eta - \frac{\nu}{4}U^2 \right)^2 \right) = \omega^2 P^2. \quad (4)$$

Stability of admissible solutions can be assessed using two Routh-Hurwitz conditions

$$64\Delta^2 + (4\eta - 3\nu U^2)(4\eta - \nu U^2) \geq 0, \quad (5a)$$

$$\nu U^2 - 2\eta \geq 0. \quad (5b)$$

Amplitudes of possible stationary solutions following Eq. (4), depending on the value of detuning  $\Delta$ , are shown in Fig. 3. The stable solutions according to the Routh-Hurwitz conditions are shown in solid lines, the unstable parts are dashed. The greyed areas denote negative values of conditions (5a,5b), respectively, i.e., the unstable regions. To complete the picture, the results from numerical simulations of the original Eq. (1) are shown in Fig. 5b. The stationary amplitudes are numerically

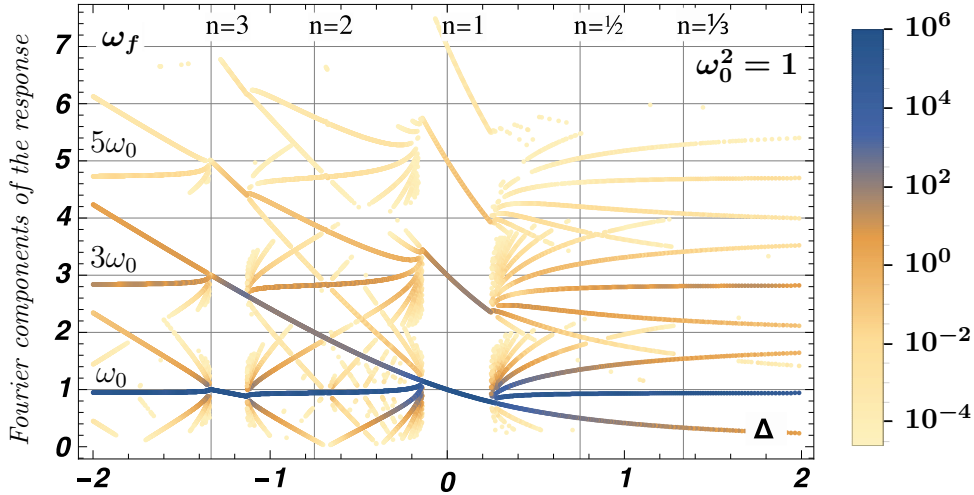


Figure 2: Frequency response characteristics of Eq. (1). The nonzero coefficients of the angular frequency are plotted versus detuning  $\Delta$ , the colour scale corresponds to the absolute values of the respective Fourier coefficients. Values used:  $\eta = 1$ ,  $\nu = 0.5$ ,  $\omega_0 = 1$ ,  $P = 1$ .

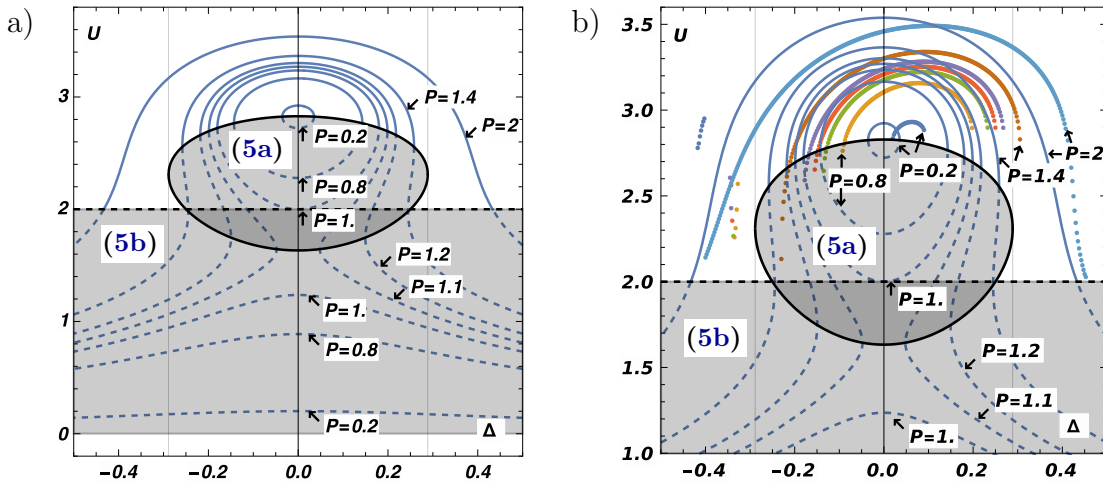


Figure 3: Theoretical amplitudes  $U$  of the harmonic solution given by Eq. (4) depending on detuning  $\Delta$ . Left: stationary amplitudes for different values of the excitation parameter  $P$ ; right: detailed view together with results from numerical simulations, indicated as colour dots. Values used:  $\eta = 1$ ,  $\nu = 0.5$ ,  $\omega = 1$ .

identified as those, where the variance of local maxima of the response for fixed values of  $\Delta, P$  is lower than certain threshold. The numerical results appear to incline to the positive values of detuning  $\Delta$ , however, the global tendency respects the theoretical mono-harmonic results.

The stationarity condition for the phase shift,  $\dot{\varphi} = 0$  in Eq. (3b), introduces a limit value of detuning

$$\Delta_0 = \frac{\omega P}{2U_0}, \quad \text{such that} \quad \cos \varphi_0 = \frac{\Delta}{\Delta_0}, \quad (6)$$

which indicates the state when the phase shift in Eq. (3b) vanishes for  $U_0^2 = 4 \frac{\nu}{\eta}$ . This amplitude corresponds to the horizontal tangent at the top of the region defined by condition (5a). When  $\Delta$  value varies, the sign of the phase shift changes when crossing  $\Delta_0 = \pm \frac{1}{4} P \omega \sqrt{\nu/\eta}$ .

The stationary solution exists for the detuning up to value  $\Delta_s$ , which is given by the condition of existence of a real solution of Eq. (4). The discriminant of Eq. (4) represents a cubic polynomial equation in  $\Delta^2$ :

$$\left( 64 (12\Delta^2 - \eta^2)^3 + (288\Delta^2\eta + 8\eta^3 - 27\nu P^2\omega^2)^2 \right) = 0, \quad (7)$$

which can have up to three real roots. The largest of these, if it exists, defines the boundary detuning of  $\Delta_s$ , depending on the system and excitation parameters. Unfortunately, there is no simple expression for  $\Delta_s$ . From the root of the discriminant with respect to  $P^2\omega^2$  of Eq. (7), it is possible to find the limiting excitation value for which Eq. (7) is applicable, i.e.,

$$P\omega \geq \frac{4\eta\sqrt{2}}{3\sqrt{3}} \sqrt{\frac{\eta}{\nu}}. \quad (8)$$

The limiting amplitude for the values used in Fig. 3 would be  $P = 1.53$ . For larger values of excitation  $P\omega$ , the existence of a stable stationary solution is governed only by the RH condition (5b). In such a case, the ‘‘ultimate’’ limit  $\Delta_{s2}$  follows from Eqs. (4,5b):

$$\Delta_{s2} = \frac{1}{2\sqrt{2}} \sqrt{\frac{\nu}{\eta}} \sqrt{P^2\omega^2 - \frac{\eta^3}{2\nu}}. \quad (9)$$

The role of the detuning limit value  $\Delta_s$  becomes apparent also when a general non-stationary solution to Eq. (3) is assumed. In such a case, after integration

$$\Delta^2 > \Delta_s^2, \quad \varphi = 2 \arctan \left( \frac{\Delta - \Delta_s}{D} \tan \frac{1}{2} Dt \right), \quad (10a)$$

$$\Delta^2 < \Delta_s^2, \quad \varphi = 2 \arctan \left( \frac{D(1 - e^{Dt})}{2\Delta} \right), \quad (10b)$$

where  $D = \sqrt{|\Delta_s^2 - \Delta^2|}$  and (without loss of generality)  $t_0 = 0$  has been assumed. The phases in Eqs. (10) represent the asymptotically constant (10b) and periodic

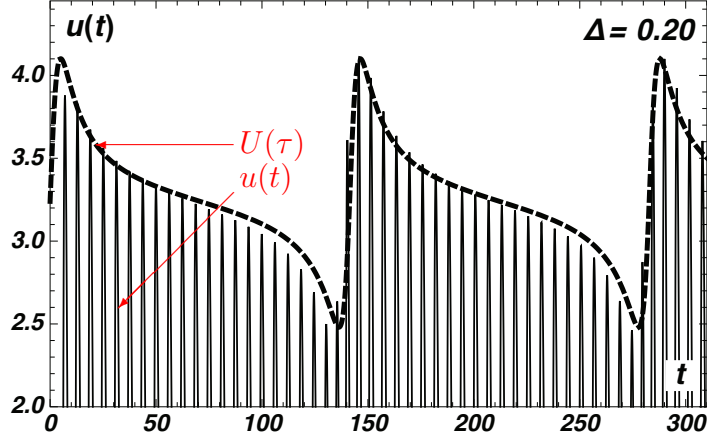


Figure 4: Time plot of numerical solution  $u(t)$  and analytical amplitude  $U(\tau)$  calculated from Eqs. (10b).

solutions (10a), which represent the stationary and nonstationary amplitudes, respectively. The amplitude can be finally enumerated from Eq. (3).

Figure 4 shows the agreement between numerical and analytical solutions that can be achieved when the initial conditions are carefully matched. In general, however, the agreement is not so good, as it was shown in Fig. 3b. This implies that, if necessary, a multi-harmonic Ansatz for the harmonic balance method or different levels of the perturbation method must be used to obtain more accurate results.

### 2.3. Analysis based on the multiple scales method

An alternative analytic approach is based on the multiple scales method, [1, 4, 3]. For this purpose, Eq. (1) will be rewritten so that its nonlinear term can be treated as a small quantity

$$\ddot{u} - \epsilon(\eta - \nu u^2)\dot{u} + \omega_0^2 u = P\omega^2 \cos \omega t, \quad (11)$$

where  $\epsilon$  is assumed to be a small parameter,  $\epsilon \ll 1$ . The solution will then be sought in the form of an expansion combining the slow and fast time scale:

$$u(t) \rightarrow u_0(T_0, T_1) + \epsilon u_1(T_0, T_1), \quad T_k \rightarrow \epsilon^k t. \quad (12)$$

Substituting Eq. (12) into (11) and comparing coefficients of similar powers of  $\epsilon$ :

$$\epsilon^0: \frac{d^2 u_0}{dT_0^2} + \omega_0^2 u_0 = P\omega^2 \cos(t\omega) \quad (13a)$$

$$\epsilon^1: \frac{d^2 u_1}{dT_0^2} + \omega_0^2 u_1 = \frac{du_0}{dT_0} (\nu u_0^2 - \eta) - 2 \frac{d^2 u_0}{dT_0 dT_1}. \quad (13b)$$

For the homogeneous case ( $P = 0$ ),  $u_0$  satisfying Eq. (13a) can be written as

$$u_0 = A(T_1) e^{i\omega_0 T_0} + \overline{A(T_1) e^{i\omega_0 T_0}}, \quad (14)$$

where  $A$  is the function to be determined. The condition of avoiding secular terms in  $u_1$  yields

$$A(T_1) (\nu A(T_1) \bar{A}(T_1) - \eta) + 2A'(T_1) = 0. \quad (15)$$

Writing  $A(T_1) = \alpha(T_1)e^{i\beta(T_1)}$  for real functions  $\alpha, \beta$ , the stationary ( $A'(T_1) = 0$ ) response amplitude agrees for  $\eta > 0$  with the parallel solution to Eq. (4):

$$u_0(t) = 2\sqrt{\frac{\eta}{\nu}} \cos(\omega_0 t) \quad \text{and} \quad u_1(t) = -\sqrt{\frac{\eta}{\nu}} \frac{\eta}{4\omega_0} \sin(3\omega_0 t). \quad (16)$$

For  $P > 0$ , the analogy of Eq. (14) reads

$$u_0 = i\Omega_p e^{i\omega T_0} - i\Omega_p e^{-i\omega T_0} + A(T_1)e^{i\omega_0 T_0} + \overline{A(T_1)}e^{-i\omega_0 T_0}; \quad \Omega_p = \frac{P}{2(\omega^2 - \omega_0^2)} \quad (17)$$

Then, the RHS in Eq. (13b) for  $u_1$  comprise the following components

$$\begin{aligned} & \kappa_1 e^{iT_0\omega} + \kappa_2 e^{iT_0\omega_0} + \kappa_3 e^{iT_0(2\omega+\omega_0)} + \kappa_4 e^{iT_0(\omega+2\omega_0)} + \\ & + \kappa_5 e^{iT_0(2\omega-\omega_0)} + \kappa_6 e^{iT_0(\omega-2\omega_0)} + \kappa_7 e^{3iT_0\omega_0} + \kappa_8 e^{3iT_0\omega} + \\ & + \text{complex conj. terms} \end{aligned} \quad (18)$$

where it has been denoted

$$\begin{aligned} \kappa_1 &= \omega\Omega_p (\nu (2|A(T_1)|^2 + \Omega_p^2) - \eta), \\ \kappa_2 &= -i\omega_0 (2A'(T_1) + A(T_1) (\nu |A(T_1)|^2 - \eta + 2\nu\Omega_p^2)), \\ \kappa_3 &= i\nu\Omega_p^2 (2\omega + \omega_0) A(T_1), & \kappa_4 &= \nu\Omega_p (\omega + 2\omega_0) A(T_1)^2, \\ \kappa_5 &= i\nu\Omega_p^2 (2\omega - \omega_0) \bar{A}(T_1), & \kappa_6 &= \nu\Omega_p (\omega - 2\omega_0) \overline{A(T_1)}^2, \\ \kappa_7 &= -i\nu\omega_0 A(T_1)^3, & \kappa_8 &= -\nu\omega\Omega_p^3. \end{aligned}$$

For the non-resonant solution in the first approximation, the elimination of secular terms reduces to the condition

$$\kappa_2 = 0. \quad (19)$$

Assuming again  $A = \alpha e^{i\beta}$  and expanding real and imaginary parts of Eq. (19) one obtains

$$\alpha = 0, \pm \sqrt{\frac{\eta}{\nu} - \Omega_p^2}, \quad \beta = k\pi, \quad k \in \mathbb{Z}. \quad (20)$$

The solution  $\alpha = 0$  is stable in the vicinity of the resonance, but is not applicable there due to the unmet assumptions. The non-zero value of  $\alpha$  applies only at some distance from the eigenfrequency, where the expression below the square root becomes positive. This later case, when substituted into Eq. (17), gives

$$u_0 = -\frac{P\omega^2}{\omega^2 - \omega_0^2} \sin(t\omega) - \frac{2}{\omega^2 - \omega_0^2} \sqrt{\frac{\eta}{\nu} (\omega^2 - \omega_0^2)^2 - \frac{1}{2}P^2\omega^4} \cos(t\omega_0). \quad (21)$$

The other option,  $\alpha = 0$ , would nullify the coefficient  $\sin(\omega_0 t)$  in Eq. (21). This way the quasiperiodic character of  $u_0$  will appear only when the non-zero  $\alpha$  attains the real value, i.e., for  $\eta/\nu > \Omega_p^2$ . Due to different assumptions used in the multiple scales method, this condition does not correspond exactly to  $\Delta_s$  defined above, however, except for a factor of  $2^{-1/2}$ , it captures  $\Delta_0$  defined in Eq. (6).

The correction term  $u_1$  would involve elimination of more secular terms originating from sub-/super-harmonic cases when  $\omega \approx 1/3\omega_0, 1/2\omega_0, 2\omega_0, 3\omega_0$ , etc., and their combinations; this is, however, out of scope of the current work.

### 3. Conclusions

A simple van der Pol deterministic system with a harmonic right-hand side was studied in the vicinity of the resonance. In addition to the previously reported results, the boundaries of the lock-in region due to the primary resonance were derived using the harmonic balance method. A limited complementary analysis based on the multiple scales method was also presented. It turns out that the weakness of the harmonic balance method is its link to the specific frequency that is assumed in the solution. In this respect is the multiple scales method more flexible because it allows more resonant frequencies to be identified in the solution. On the other hand, the use of the multiple scales method is limited to the assumption of small nonlinearity, which can be limiting in some cases. In both approaches, a more detailed analysis will have to be adopted in order to qualitatively assess the fine details of the quasiperiodic processes surrounding the resonance region.

### Acknowledgement

The support of CSF project 21-32122J and RVO 68378297 support are acknowledged.

### References

- [1] Afzali, F., Kharazmi, E., and Feeny, B.F.: Resonances of a forced van der Pol equation with parametric damping. In: *NODYCON Conference Proceedings Series*, pp. 477–487. Springer International Publishing, 2021.
- [2] Gardner, W. and Franks, L.: Characterization of cyclostationary random signal processes. *IEEE Transactions on Information Theory* **21** (1975), 4–14.
- [3] Nayfeh, A.H.: *Perturbation Methods*. Wiley, 2000.
- [4] Nayfeh, A.H. and Mook, D.T.: *Nonlinear Oscillations*. Wiley, 1995.
- [5] Náprstek, J. and Fischer, C.: Analysis of the quasiperiodic response of a generalized van der Pol nonlinear system in the resonance zone. *Computers & Structures* **207** (2018), 59–74.
- [6] Náprstek, J. and Fischer, C.: Super and sub-harmonic synchronization in generalized van der Pol oscillator. *Computers & Structures* **224** (2019), 106–103.